Original research article

Role of harvest depth filtration in controlling product-related impurities for a bispecific antibody

Ehsan Espah Borujeni[1],[†], Weixin Jin[1],[†], Chun Shao[2], Naresh Chennamsetty[3], Xuankuo Xu[1],* 🆔 **and Sanchayita Ghose[1]**

[1]Biologics Downstream Process Development, Bristol Myers Squibb, Devens MA 01434, USA , [2]Global Process Analytical Science, Bristol Myers Squibb, Devens MA 01434, USA , and [3]Analytical Development and Attribute Sciences, Bristol Myers Squibb, New Brunswick NJ 08903, USA

ABSTRACT

Background: Bispecific antibodies (BsAb) belong to a novel antibody category with advantages over traditional mono-specific therapeutic antibodies. However, product variants are also commonly seen during the production of BsAb, which poses significant challenges to downstream processing. In this study, the adsorptive characteristics of a BsAb product and its variants were investigated for a set of depth filters during primary recovery of the cell culture fluid. Methods: The retention of the BsAb product and its variants on a set of Millistak+® D0HC and X0HC depth filters were first investigated, followed by studying the mechanism of their adsorption on the depth filters. The chemical and structural properties of depth filters along with the molecular properties of the product and its variants were studied subsequently. Results: The X0HC filter was found to be able to retain a significant amount of low molecular weight (LMW) variants along with a low amount of main product retained. Different levels of retention, observed for these variants, were correlated to their different hydrophobic and charge characteristics in relation with the adsorptive properties of the depth filters used. Electrostatic, hydrophobic, and hydrogen bonding interactions were found to be the key forces to keep product variants retained on the depth filter where the higher hydrophobicity of the LMW variants may cause them to be preferentially retained. Conclusion: Harvest depth filters potentially can be utilized for retaining the BsAb variants, which depends on relative molecular properties of the product and its variants and adsorptive properties of the depth filters used.

Statement of Significance: This work for the first time demonstrates that the harvest depth filters can retain product-related impurities of bispecific antibodies (particularly LMW) through hydrogen bonding, hydrophobic, and electrostatic interactions. The experimental framework used here can be applied to investigation of the filter binding mechanism for other therapeutic modalities.

INTRODUCTION

Bispecific antibodies (BsAb) belong to a novel antibody category that simultaneously binds to two different epitopes or targets, making this class of therapeutics advantageous over traditional mono-specific antibodies. Thus, the growing interest in designing and developing this type of therapeutics has led to more than 110 BsAb candidates in clinical trials and three BsAb products already marketed to date [1]. There have been more than 50

(HIC) [6, 7], and mixed-mode chromatography (MMC) [8, 9] to remove BsAb product-related impurities.

Depth filtration is commonly employed in biologics purification processes to primarily remove insoluble particles, whereas its ability to remove soluble impurities has been reported with relatively limited mechanistic understanding [10–12]. The harvest depth filters of various nominal pore size ratings are usually designed to retain cells and cell debris in a wide range of sizes. In addition,

---

*To whom correspondence should be addressed. Xuankuo Xu, Biologics Downstream Process Development, Bristol Myers Squibb, 38 Jackson Rd, Devens, MA 01434, USA. Fax: +1 978-588-6293; Tel: +1 978-588-3056; Email: xuankuo.xu@bms.com
†First authors with equal contribution

depth filters with certain adsorptive characteristics may help retain process-related impurities such as host cell proteins (HCPs) [11, 13, 14] and DNA [15], as well as undesired product-related impurities such as high or low molecular weight (HMW, LMW) variants. For example, application of a set of Millistak+® D0HC and X0HC depth filters to remove HMW and LMW variants of a mAb during the harvest process has been previously reported [16]. Using molecular modeling, Yu *et al*. [16] attributed the retention of these product-related impurities to the hydrophobic interactions (HICs) with the filter media with minimal impact of electrostatic interactions during harvest filtration, while systematic experimental investigation of the binding mechanism was still lacking.

In this work, we studied the capability of Millistak+® D0HC and X0HC depth filters to retain LMW fragments of a BsAb molecule (called BsAb1 here) during the harvest process. The retention of LMW variants along with the product on the depth filters was evaluated with a set of experiments to directly investigate the adsorption mechanism on the filters. The molecular properties of the product and its variants were then evaluated to explain the adsorption data obtained. The strength and mechanism of the variants binding to the filters were affected by the properties of the molecules involved as well as the characteristics of the filters used. Therefore, understanding these properties can facilitate the design of a robust depth filtration process for retention of soluble impurities. To our knowledge, this is the first study on the application of depth filtration to removing undesired product variants during a BsAb purification process.

MATERIALS AND METHODS

Materials

Cell culture fluid (CCF) and drug substance (DS) of BsAb1 were produced at Bristol Myers Squibb using standard manufacturing procedures. The purified BsAb1 product used in the experiments were obtained by buffer exchanging of BsAb1 DS into the desired buffer conditions. Millistak+® μPod D0HC and X0HC depth filters were purchased from MilliporeSigma. Reagents were obtained from Thermo Fisher Scientific unless otherwise specified. All experiments were performed at room temperature of 20–25°C.

Depth filtration experiments

A qualified scale-down depth filtration model was established to study the impact of process parameters on the removal of process and product-related impurities for the D0HC and X0HC filters using the same surface area ratio as that for manufacturing operation. The scale-down experiments were performed using 23 cm² capsules of the D0HC and X0HC filters connected in series. The ratio of primary (D0HC) to secondary (X0HC) filter surface area was 1:1. Prior to use, the entire filter train was flushed using 100 L/m² of water for injection, based on total filter area, at a flux of 300–600 (L/m²/h) (LMH). Then, the

CCF was loaded onto the depth filters. The system hold-up volume with the confirmed absence of product was discarded before collecting the product pool to avoid unnecessary pool dilution. The targeted feed flux during filtration was at 50 LMH, and the load capacity was controlled at 70 L/m². The pressure limit for the system was set to 20 psi. A chase flush was performed using phosphate-buffered saline (PBS) buffer (i.e., 20 mM NaH_2PO_4, 150 mM NaCl pH 7.2) to recover the product after loading was finished. During depth filtration, the filtrate was collected either as a bulk solution into a tared bottle sitting atop a balance or into separate fractions.

Some filtration experiments were conducted using purified BsAb1 product or centrifuged CCF (supernatant of cell culture centrifuged for 10 min at 3000 *g*). Those experiments were performed with the pre-flushed depth filter(s) mounted on the ÄKTA Avant 150 system and the filtrate collected in intervals of 10 L/m² after UV280 nm reached 50 mAU. Once the target filter loading was achieved, the depth filters were chased with PBS buffer. In selected experiments, the filters were further flushed with different buffers to investigate the mechanism of BsAb1 and its variants adsorption to the depth filters. Furthermore, 0.1 N NaOH was used to further recover the bound material on the filters. Fifty LMH flux was maintained throughout the experiment.

Reduced and non-reduced SDS-PAGE analysis

Reduced and non-reduced Sodium dodecyl-sulfate polyacrylamide gel electrophoresis (SDS-PAGE) were used to visualize product relevant variants in centrifuged CCF or purified product samples. About 4–20% mini-PROTEAN TGX stain-free protein gel (BIO-RAD Cat# 4568093) was used to separate proteins under reduced and non-reduced conditions. Premixed 4× Laemmli protein sample buffer for SDS-PAGE (Cat#1610747) and protein standard (Cat#1610363) were also purchased from Bio-Rad. NOVEX Tris-Glycine SDS running buffer (10×) was purchased from Thermo Fisher Scientific (Cat#LC2675).

Samples containing 10–25 μg of total protein were mixed with 4× Laemmli protein sample buffer and 50 mM fresh Dithiothreitol (DTT) and incubated at 95°C for 5 min before loading for reduced SDS-PAGE. For non-reduced SDS-PAGE, samples were mixed with 4× Laemmli protein sample buffer before loading. Electrophoresis was carried out at a constant voltage of 150 V for 1.0 h or until the blue dye moved to the bottom edge. The gel was then visualized with UV-light with the BIO-RAD ChemiDoc MP Imaging System. The semi-quantitative processing of the gel image was also done using the software associated with the ChemiDoc MP Imaging System.

Relative surface hydrophobicity analysis

The relative surface hydrophobicity of the product and its variants were evaluated experimentally using an analytical HIC method following a protocol [11] with a minor modification of the mobile phase. Samples were analyzed using a TOSOH Bioscience® TSKgel Butyl-NPR column

(4.6 mm × 10 cm, Tokyo, Japan) run on a Waters 2695 system with a 2298 PDA detector (Agilent Technologies, Santa Clara, CA). The column was initially equilibrated with 0.1 M phosphate buffer containing 0.8 M ammonium sulfate at pH 7.0. Samples subjected to HIC analysis were diluted to 0.5 mg/mL with the equilibration buffer. Approximately 12 μg of sample was injected per run using an autosampler, with the proteins eluted using a linear gradient of the equilibration buffer and 0.1 M phosphate buffer, varying from 100 to 0% ammonium sulfate over 30 min. Columns were run at a constant flow rate of 0.35 mL/min, with proteins detected by UV absorbance at 280 nm.

Liquid chromatography-mass spectrometry (LC–MS)

Samples were diluted to 1 mg/mL using Optima™ LC-MS water grade (Fisher Scientific, Cat#W6-1) and loaded to a Waters Acquity I-Class UPLC system for injection. Protein (10 μg) was loaded to a BioResolve RP mAb Polyphenyl Column (450 Å, 2.7 μm, 2.1 mm × 150 mm) (Waters—Cat#176004157) followed by a gradient change of mobile phase A (0.05% Trifluoroacetic Acid, from Fisher Scientific, Cat#A116-10X1AMP) and mobile phase B (Acetonitrile (ACN), from Fisher Scientific, Cat# A955-1) at a flow rate of 0.3–0.5 mL/min. Column was running at 80°C for intact mass spectrometry analysis using Q Exactive Orbitrap mass spectrometer (Thermo Fisher Scientific). The intact mass analysis was performed using Protein Metric (PMI) software.

Size-exclusion chromatography

Soluble product aggregates were analyzed on a Waters HPLC system (Agilent 1100/1200) with UV detection at 280 nm. An analytical column, Tosoh TSKgel SuperSW3000, 4.6 mm × 300 mm, 4 μm was used. All samples were 0.2 μm-filtered to remove potential large particles prior to applying a total mass of 50 μg protein to the SEC-UPLC system. The mobile phase (200 mM sodium phosphate, 150 mM sodium chloride, pH 6.8) was run at a flow rate of 0.4 mL/min. Data were analyzed using Waters Empower 3 chromatography data system software (Waters, version 3).

Residual HCP measurement

HCPs were quantified using the third generation generic ELISA kit from Cygnus Technologies (Cygnus Technologies, Southport, NC) following manufacturer's instructions. The detection range is 3–100 ng/mL. Serial dilutions of samples were made to keep the measurement within the calibration range. Absorbance was measured at 450/650 nm (10 min) using Molecular Device SpectraMax plate reader and analyzed using SOFTMaxPro Version 4.6 software.

Residual DNA measurement

Residual DNA in the samples was measured using real-time quantitative PCR (RT-qPCR). PrepSEQ residual DNA Sample Preparation Kit (Life Technologies) was used to prepare samples. RT-qPCR was carried out with the 2× TaqMan Universal PCR Master Mix Kit (Life Technologies) and 7500 HT Real-Time PCR system (Life Technologies) according to the manufacturer's instructions.

Homology modeling

The 3D tertiary structure of the unique 2 + 1 format protein (Fab-Fc-Fab-Fab) was obtained by combining the 3D models for an antibody (Fab-Fc-Fab) and a separate Fab. The models for BsAb1 were built using the homology modeling protocol within Molecular Operative Environment (MOE) software (Chemical Computing Group ULC, Montreal, QC, Canada). These models were then combined with a flexible linker, and the resulting structure was subjected to a structure refinement procedure with energy minimization to relieve strained geometry. The effective protein charge as a function of pH was calculated based on the ensemble charges with titration protocol within the MOE software. The charge was modeled based on the pKa values of titratable residues, which in turn was predicted based on the electrostatic interactions of these residues to the other residues within the protein structure.

RESULTS

Retention of BsAb1 variants during harvest depth filtration

BsAb1 was a trivalent IgG1-like bispecific antibody in a 2 + 1 asymmetric format, with an isoelectric point (pI) of 7.8 and a molecular weight of 168 kDa. It contained antigen-binding regions for two different epitopes, termed "a" and "b" here. Figure 1 presents illustrative cartoons of the structures of BsAb1 molecule and its undesired variants that can be co-expressed in the cell culture. The "Fab" fragments illustrated in Fig. 1 include both the variable and constant domains of antigen-binding region of each epitope.

A lab-scale experiment using the D0HC and X0HC filter train was conducted to harvest BsAb1 CCF that was loaded up to 70 L/m² based on the D0HC filter area used. The depth filtered harvest pool (termed as "DF pool") was then analyzed along with a centrifuged CCF sample (directly from the pre-harvest cell culture broth, termed as "Centr. CCF") and a BsAb1 DS sample. Figure 2 shows the SDS-PAGE results (non-reduced in Fig. 2A and 2C, and reduced in Fig. 2B and 2D) where the sample compositions were determined semi-quantitatively based on band intensity analyses of the gel images. As seen in Fig. 2A, the "Centr. CCF" sample contained excessive amount of three major LMW variants, deemed as light chain (LC) (LMW 1), LC-dimer (LMW 2), and homodimer or other LMW variants (LMW 3) based on their corresponding molecular weights. The total LMW amount quantified in the "Centr. CCF" sample was 19%, significantly higher than that in the "DF pool" sample (7%) (Fig. 2C). The DS sample contained greater than 99% of BsAb1 monomer. Under reduced condition (Fig. 2B), the intra- and interpeptide disulfide bonds were broken, thus heavy chains (HCs) and LCs were well separated in the gel, resulting in three major bands corresponding to knob-HC (MW of ∼71 kDa), hole-HC (MW of ∼50 kDa), and the LC variants of the two target BsAb1 epitopes (a-LC and b-LC).
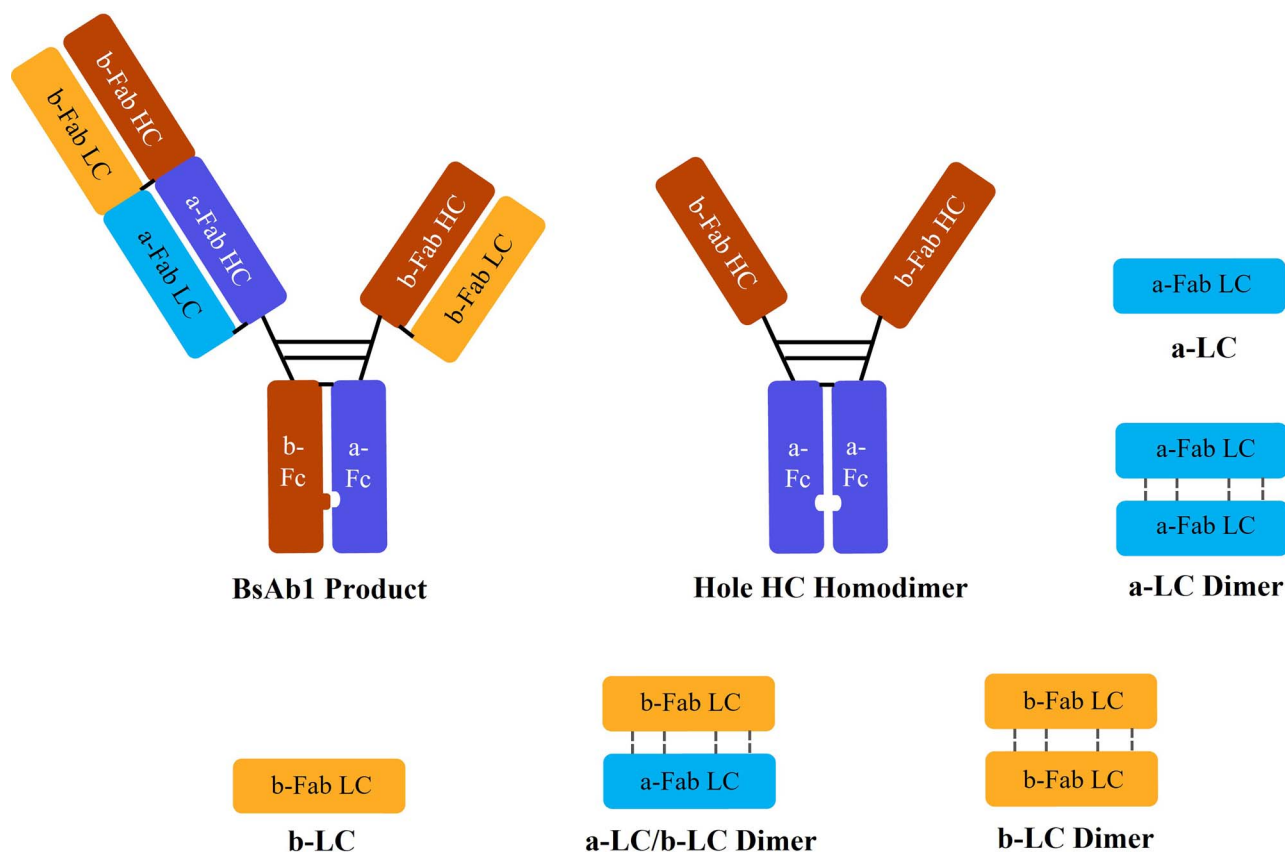
Figure 1. BsAb1 molecule and its co-expressed variants present in CCF. Solid lines represent intra- and inter-peptide disulfide bonds. The intramolecular bonds in dimer variants are unknown and shown by dashed line for illustration purposes only.

Due to their similar sizes (MWs of ∼ 25 kDa), a-LC and b-LC appeared as one band in the reduced gel image. It should be noted that, despite the similar band migration pattern, the highest LC content was seen in the "Centr. CCF" sample (Fig. 2D), indicating that the amounts of the LCs differed considerably among the samples. This observation agreed very well with the non-reduced condition results (Fig. 2C).

To further confirm the identity of the species seen in Fig. 2, the "Centr. CCF" and "DF pool" samples were analyzed using the LC–MS method. Figure 3 shows the product-related LMW variants labeled on the UV280 nm chromatogram from the LC–MS analysis. In both samples, there were five major distinct peaks corresponding to monomer, homodimer, a-LC dimer, a-LC, and b-LC variants of the BsAb1 molecule. Noticeably, the peaks associated with the LMW variants of the "DF pool" sample, particularly a-LC and a-LC dimer, were smaller than those of the "Centr. CCF" sample (i.e., total LMW composition of 7.8% vs. 18.5%, respectively), indicating their reduced amounts due to the D0HC/X0HC depth filtration during the harvest operation. These results were consistent with the LMW levels obtained from the non-reduced SDS-PAGE analysis (Fig. 2C). However, the peaks associated with the hole-HC homodimer variant in the "Centr. CFF" and "DF pool" samples were of similar size, suggesting negligible retention of this variant during depth filtration.

This observation was not in agreement with the SDS-PAGE image under non-reduced condition, shown in Fig. 2A, where the hole-HC homodimer was also partially removed during depth filtration. This discrepancy was due to co-presence of other LMW variants along with the homodimer under the associated LC-MS peak, which led to inaccurate quantification of the homodimer based only on the peak size. It should also be noted that in Fig. 3 there were several minor peaks attributed to other LMW variants associated with the b-LC of BsAb1 (i.e., b-LC, b-LC dimer, b-LC/a-LC dimer). These LMW variants likely co-migrated along with the a-LC and a-LC dimer under the non-reduced SDS-PAGE condition due to their similar sizes, leading to one LMW1 and one LMW2 band in Fig. 2A. Figure 3 also indicates that these low-abundance LMW variants had relatively negligible retention on the depth filters evaluated. Therefore, the following study was primarily focused on the major LMW variants (i.e., a-LC, a-LC dimer, and homodimer) that were effectively reduced through the D0HC/X0HC filtration. In addition, it should be noted that there were other unidentifiable species, (e.g., cell culture media components), with elution times between t = 4 and t = 7 min in Fig. 3. They composed a total of 7.1% of "Centr. CCF" sample but were reduced to 1.9% composition in "DF Pool". Since the amount of these species was negligible, characterizing these species was outside the scope of this study. Overall, the data clearly show
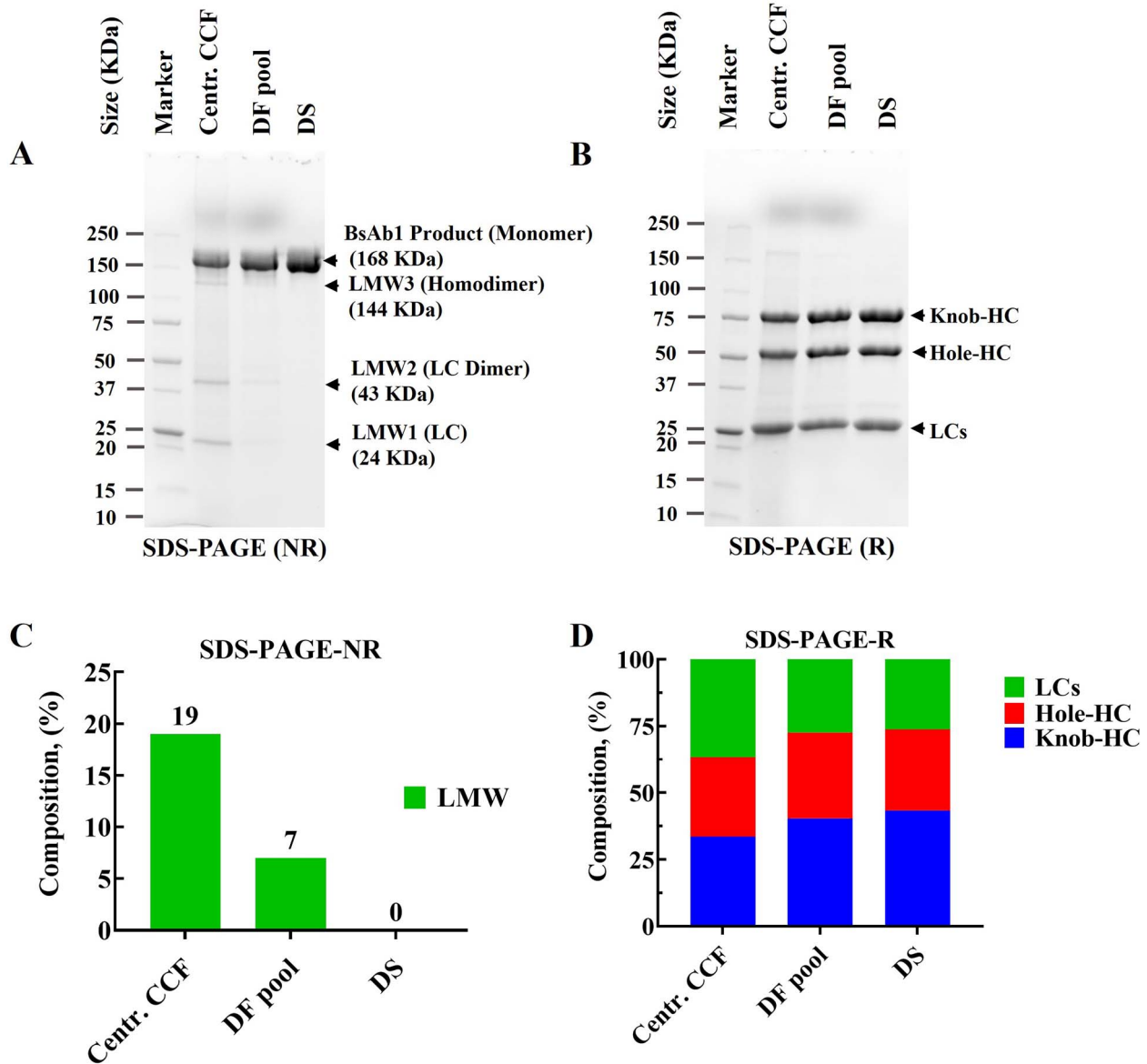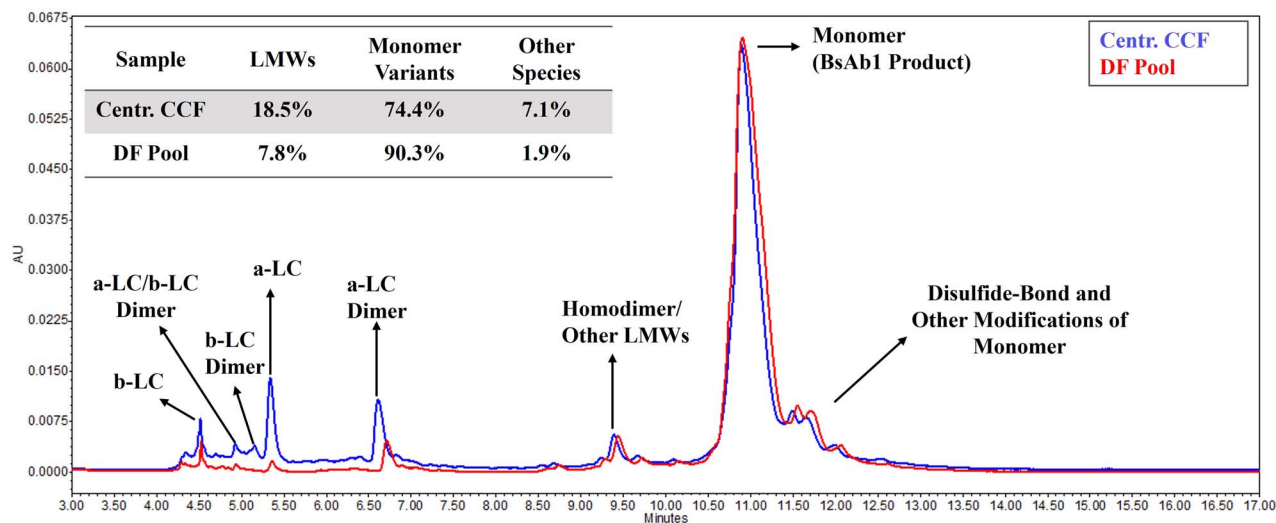
Figure 2. SDS-PAGE images of the "Centr. CCF" and "DF Pool" samples obtained in BsAb1 harvest depth filtration using the D0HC/X0HC filter train under (A) non-reduced and (B) reduced conditions. Band intensity analysis for composition of (C) LMWs under non-reduced and (D) LCs and HCs under reduced conditions.

that the depth filters could alter the composition of the BsAb1-related LMW variants present in the CCF due to their different retention properties, potentially reducing the burden of impurities removal in subsequent unit operations.

Retention capacity of BsAb1 variants on each depth filter

To investigate the adsorption phenomena across the D0HC and X0HC filters, two separate depth filtration experiments were conducted using centrifuged CCF obtained from a 500 L BsAb1 batch. CCF was centrifuged at 1000 *g* for 10 min with supernatant collected for the depth filtration experiments. Experiments were conducted using the D0HC filter alone and in series with the X0HC filter with

1:1 filter area ratio. The feed materials were loaded up to 70 L/m² based on the primary filter area. The permeate samples were then collected throughout both runs with their composition along with that of the feed sample analyzed using band intensity analysis of the gel images obtained from the non-reduced SDS-PAGE assay. Figure 4 shows the gel images of the permeate samples collected as a function of filter loading for both runs. Results indicate that the three major LMW variants (homodimer, a-LC and a-LC dimer) were minimally retained by the D0HC filter alone (Fig. 4A). However, these variants were retained effectively in the first few fractions of the D0HC/X0HC run (Fig. 4B), and they started gradually saturating the filters as the loading was increased, with the earliest breakthrough observed for the homodimer. Comparing the gel images

Figure 3. LC-MS UV280 nm chromatogram of the "Centr. CCF" and "DF Pool" samples obtained in a BsAb1 harvest depth filtration using the D0HC/X0HC filter train.

clearly suggests that the major retention of the LMW variants took place on the X0HC filter with negligible contribution from the D0HC filter to the retention of these variants. Figure 4C presents the composition of the LMW variants in the D0HC/X0HC filtrate determined by band intensity of the gel image in Fig. 4B and normalized with the composition of the centrifuged CCF. The a-LC and a-LC dimer variants were retained more strongly than the homodimer, with only around 33% breakthrough observed at 70 L/m² loading where the homodimer reached full breakthrough. In addition, the normalized composition of BsAb1 monomer was greater than 1.0 during filtration which demonstrates increasing purity of BsAb1 monomer achieved by preferentially retaining LMW variants on the depth filter.

The removal of process-related impurities (i.e., HCP, DNA) and HMW variants was also analyzed. HCP and DNA were reduced across both the D0HC and X0HC filters with more pronounced retention of both HCP and DNA impurities on the X0HC filter observed (data not shown). Similarly, HMW variants had higher adsorption on the X0HC filter (Fig. 4D), suggested by the minimal retention using the D0HC filter alone and the clearly delayed breakthrough for the D0HC/X0HC filter train. It should be noted that, due to very low HMW content in the in feed (~1.1%), the clearance of those LMW variants through depth filtration was the primary focus of this study. Considering that the D0HC filter showed minimal adsorption of different BsAb1 variants, the adsorption mechanism within the X0HC filter was specifically investigated in subsequent experiments.

Adsorption mechanisms of BsAb1 on the X0HC filter

Due to the difficulty in effectively isolating and enriching the LMW variants (i.e., a-LC, a-LC dimer, and homodimer) to evaluate their binding mechanism individually, the adsorption mechanism of the BsAb1 product on the X0HC filter was first investigated as a function of process conditions and molecular properties. Those molecular properties were then evaluated for BsAb1 LMW variants and compared with that of the BsAb1 product to explain the varied retention tendencies observed among the BsAb1 and its LMW variants.

The impact of electrostatic interactions was studied through a set of experiments using purified BsAb1 materials, obtained by buffer exchanging BsAb1 DS into phosphate buffers (i.e., 20 mM NaH_2PO_4, pH 7.2) with different concentrations of NaCl. The feed materials were loaded up to 44 L/m² on the X0HC filter, followed by a chase step until the UV280 nm profile reached zero. The chase buffer in each experiment had similar ionic strength to that of the feed. Finally, the filter was flushed with 1 M NaCl to ensure the removal of species retained within the filter media by electrostatic interactions. All the steps in these runs were conducted at 50 LMH. Figure 5A presents the UV280 nm profiles of these runs, and Fig. 5B shows the product recovery during the loading and chase steps compared with that in the high-salt flush step. Increasing salt concentration in the feed led to earlier product breakthrough and more product collected in the filtrate during the loading and buffer chase steps (Fig. 5A). In addition, the amount of the recovered product using 1 M NaCl flush was decreased with increasing feed salt concentration until the recovery in the flush step became negligible (i.e., < 1% of loaded material) for the feed at ≥150 mM NaCl. These observations suggest that electrostatic interactions played an important role in the retention of the BsAb1 product; however, its contribution seemed to be minimal at ≥150 mM NaCl. Since the BsAb1 CCF materials had an ionic strength close to 150 mM NaCl, the electrostatic interactions would not seem to be a key contributor to the retention of the BsAb1 molecule on the X0HC filter during harvest depth filtration. On the other hand, even for the feed at 500 mM NaCl where the electrostatic interactions should be practically shielded,
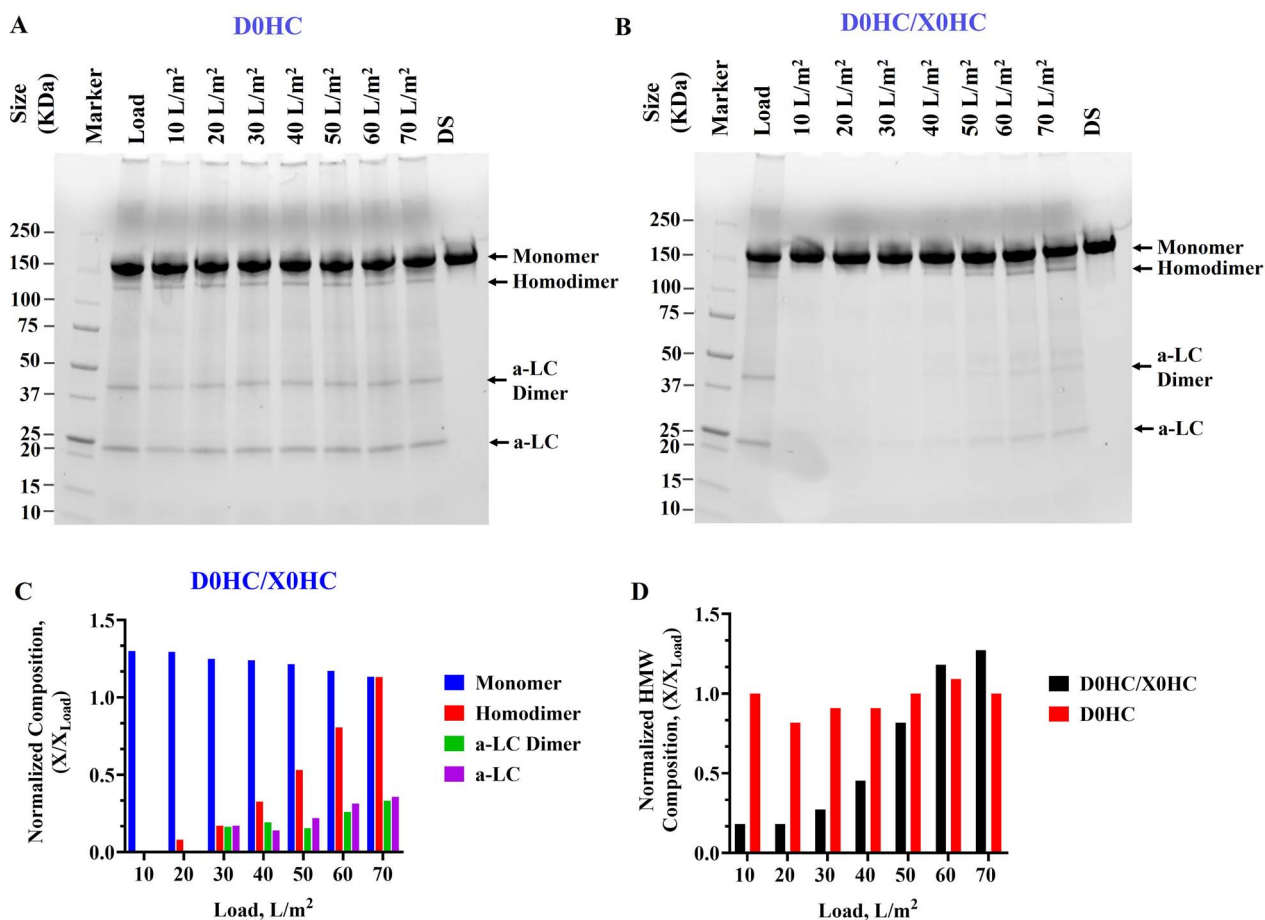
Figure 4. Non-reduced SDS-PAGE image of the permeate fractions of the BsAb1 centrifuged CCF, filtered through (A) the D0HC filter, and (B) the D0HC/X0HC filter train. Breakthrough analysis of (C) the BsAb1 product and its LMW variants through the D0HC/X0HC filter train, and (D) the BsAb1 HMW variants through the D0HC and D0HC/X0HC filter train.

only 88.5% of the total loaded material was eventually recovered with the rest remaining bound on the filter. This finding indicates that other types of adsorptive driving forces may also be involved in the retention of the BsAb1 product and its variants onto the X0HC filter media.

The contribution of hydrophobic interactions was evaluated by flushing separate pre-loaded X0HC filters using different organic solvents and measuring the amounts of recovered material in each case using UV280 nm absorbance. In these experiments, 125 g/m² of purified BsAb1 material, present in PBS buffer with 150 mM NaCl, was first loaded on each filter followed by the chase using the background buffer of the load solution. Then, each of loaded depth filters was flushed using a different organic solvent (i.e., 30% propylene glycol, 10% ethanol, and ACN with gradually increased concentration of 0–25%) aiming to remove the bound molecules retained by hydrophobic interactions. Interestingly, the amount of material recovered during the organic solvent flush in all three cases was minimal (data not shown), indicating that either the hydrophobic interactions played an insignificant role in the BsAb1 retention on the X0HC filter, or the adsorption mechanism involved complex interactions and disrupting hydrophobic interactions alone was insufficient to desorb

the bound BsAb1 molecules. Higher concentrations of these organic solvents were not used here to avoid potential denaturation of the BsAb molecules bound on the filter.

To gain further mechanistic insight into the BsAb1 binding on the X0HC filter and investigate the impact of different types of interactions, 1 M NaCl, 1 M arginine, and 2 M urea were used to flush out the bound molecules from separate pre-loaded filters. Purified BsAb1 in PBS buffer with 150 mM NaCl was used in these experiments. Urea and arginine are liquid phase modifiers with applications in chromatographic systems to improve the resolution of protein separation or to increase protein stability [17, 18]. Urea can disrupt hydrophobic interactions and hydrogen bonds, whereas arginine can modulate hydrophobic interactions and hydrogen bonds as well as electrostatic interactions via different subunits in its structure (i.e., methylene, guanidine, and carboxylate groups) [19, 20]. Table 1 shows the product recovery achieved in each experiment along with the structures of urea and arginine which led to multimodal intermolecular interactions. Results suggest that the contribution of electrostatic interactions alone was negligible due to the relatively high salt concentration present in the feed stream which led to only 0.9% of the filtered product recovered in the 1 M NaCl flush pool. When 2 M urea was

A

B
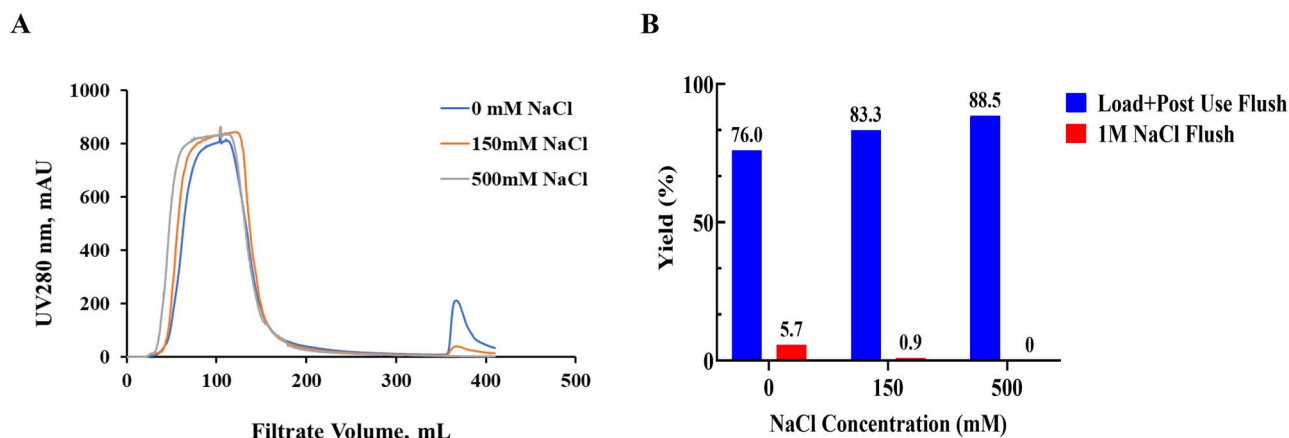
Figure 5. The effect of electrostatic interaction on adsorption of the purified BsAb1 product, present in PBS buffer with different NaCl concentrations, on the X0HC filter. (A) UV280 nm chromatogram of permeate flowthrough during the load, chase, and high-salt flush steps. (B) Product recovery in different steps of filtrations.

Table 1. Recovery of the purified BsAb1 product adsorbed on the X0HC filter using salt and mobile phase modifiers

| Flush buffer	Modifier structure	Recovery during load and chase (%)	Recovery during flush (%)	Unrecovered (%)
1 M NaCl	N/A	83.3	0.9	15.8
2 M Urea		83.0	4.7	12.3
1 M Arginine		83.9	10.1	6.0
2 M Urea +1 M NaCl	N/A	85.2	7.8	7.0

used, 4.7% of the filtered product was recovered indicating that hydrogen bonding and hydrophobic interactions together possibly played a role in adsorbing the BsAb1 molecules and in the ineffectiveness of desorbing the bound protein by only disrupting the hydrophobic interactions, as shown in the earlier flush study using organic solvents. Flushing the depth filter with 1 M arginine resulted in recovering 10.1% of the filtered product which was the highest compared with that obtained using 1 M NaCl and 2 M urea. This finding is aligned with the known property of arginine to simultaneously weaken electrostatic, hydrophobic, and hydrogen binding interactions. When a pre-loaded depth filter was flushed using a combined solution containing 2 M urea and 1 M NaCl, the amount of recovered product was 7.8%, higher than that obtained from using each buffer separately, indicating potential synergistic effects and a complex mechanism involved in the system studied here. It should be noted that around 3–6% of the filtered product was irreversibly bound to the filter and remained unrecoverable even after an additional flush using 0.1 N NaOH.

Molecular properties of BsAb1 and its variants

Surface hydrophobicity and charge characteristics of the BsAb1 product and the LMW variants were assessed to explain the higher retention of these LMW variants on the X0HC filter initially observed during harvest of the BsAb1 CCF. Figure 6A shows the calculated net effective charge of the BsAb1 product, a-LC, and homodimer variants as a function of pH using MOE software. The charge properties of the a-LC dimer were not evaluated here due to its unknown structure. With very similar pI, the BsAb1 product was strongly positive (+11.4) compared with the homodimer (+2.9) and the a-LC (+1.3) at the pH (7.2) of the CCF; however it only led to limited adsorption of the BsAb1 product on the negatively charged elements of the X0HC filter media [21] at the relatively high salt concentration. Therefore, electrostatic interactions likely played very little role in retaining the a-LC variant due to its negligible positive charge.

The analytical HIC assay was applied to assess the relative surface hydrophobicity of these species using an LMW-enriched sample from a strip pool of a chromatography

A

C

B
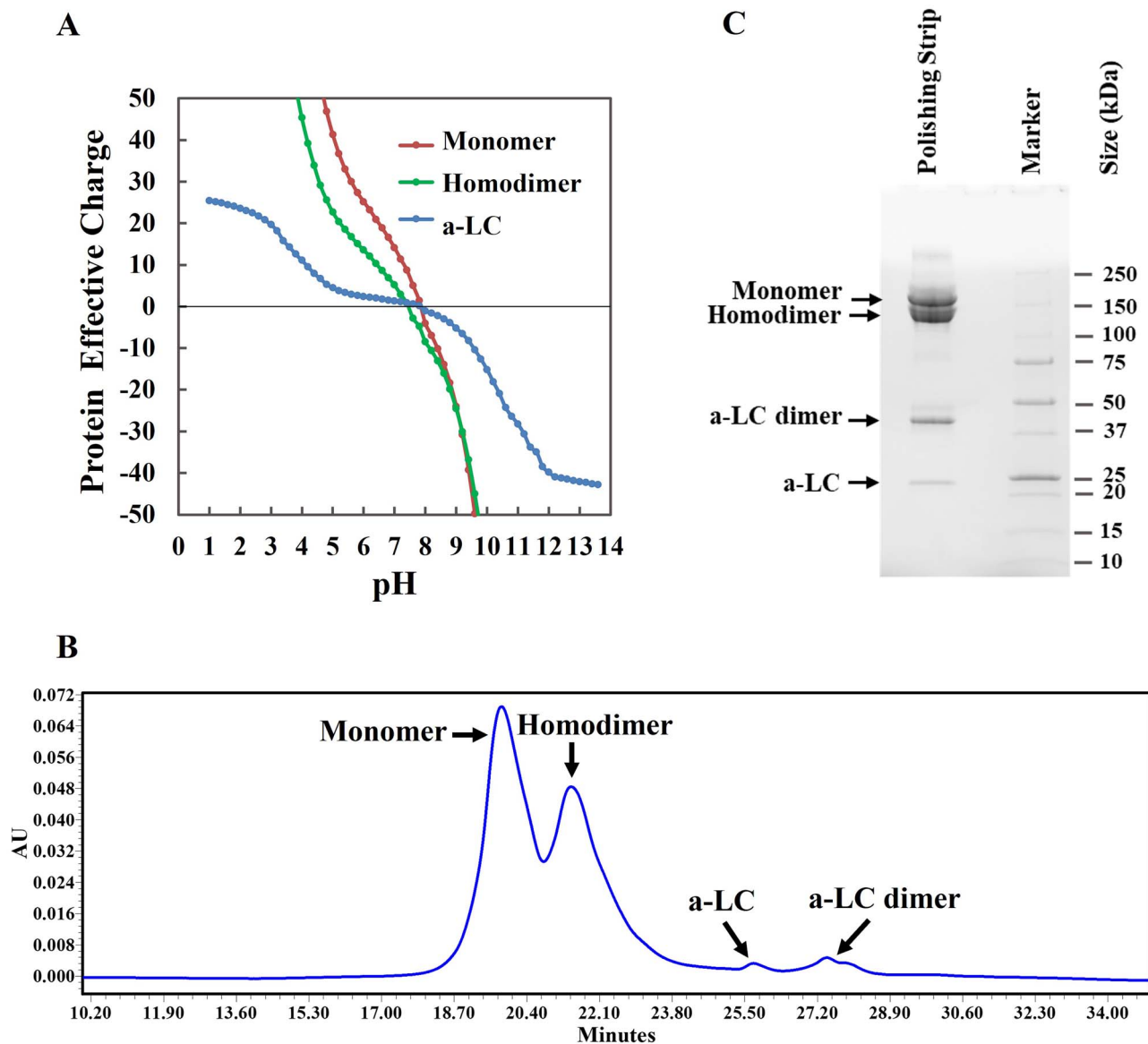
Figure 6. Surface hydrophobicity and charge characteristics of the BsAb1 product compared with its LMW variants. (A) Calculated net effective charge as a function of pH, and (B) UV280 nm chromatogram of the analytical HIC assay obtained for relative surface hydrophobicity evaluation.

polishing step ("Polishing Strip") in the BsAb1 downstream process. The HIC chromatogram in Fig. 6B shows four major peaks corresponding to the BsAb1 product-related species, consistent with the bands seen in the non-reduced SDS-PAGE image in Fig. 6C, as expected for the BsAb1 monomer and three LMW variants. The amounts of process-related impurities (e.g., HCP and DNA) in the "Polishing Strip" sample were confirmed to be negligible with minimal interference with the HIC assay. The sample was analyzed by the LC–MS method (data not shown) to determine the identity of the peaks in Fig. 6B based on the relative sizes of the LC–MS peaks. The peak for the BsAb1 monomer in the HIC chromatogram was eluted first (i.e., 19.81 min retention time), indicating that the BsAb1 monomer was less hydrophobic than the LMW variants studied. The homodimer forms appeared to be slightly

more hydrophobic than the BsAb1 monomer, whereas the a-LC dimer was the most hydrophobic followed closely by the a-LC. The relative hydrophobicity data agreed well with the results in Figs 2A and 3 where the a-LC and a-LC dimer were shown to be more retained than the BsAb1 monomer on the X0HC filter, suggesting the potential critical role of hydrophobic interactions. This finding is aligned with other reported work [16] that attributed the binding of product-related impurities (HMW and LMW) for a mAb to hydrophobic interactions with the X0HC filter.

DISCUSSION

The results presented above demonstrate that the BsAb1 product and its variants were retained on the X0HC filter

through a complex mechanism mainly involving electrostatic, hydrophobic, and hydrogen bonding interactions. This multimodal mechanism can be attributed to both the filter characteristics determined by structural complexity and heterogenous properties, and the protein characteristics including the surface properties (e.g., size, hydrophobic, and charged patch distribution, etc.) of the BsAb1 product and its related variants. Depth filters used in bioprocesses are usually composed of a heterogenous mixture of fibrous backbone (commonly made of cellulosic material), synthetic or naturally derived filter aids, and charged polymeric binders that hold all the elements together and provide structural support to the filter media. Wide application of depth filtration in bioprocessing has led to an increasing number of studies evaluating structural properties of different commercially available depth filters and the retention mechanisms for soluble impurities.

The properties of the Millistak+® D0HC and X0HC filters have been recently investigated using confocal microscopy [21]. It was shown that the X0HC filter is composed of two layers both containing mainly naturally derived diatomaceous earth (DE) filter aids and a small portion of cellulosic fibers. However, very little comment was made on the presence of polymeric binders in these layers. On the other hand, the D0HC filter was shown to be composed of two layers with higher cellulosic fiber and lower DE contents than those of the X0HC filter. This variation likely leads to larger nominal pore size and thus smaller binding surface area in the D0HC filter than the X0HC filter. The larger pore size of the D0HC filter also potentially leads to less proximity of binding sites which reduces the chance of multiple interactions between the bound species and the filter media. In addition, the adsorptive properties of these two filters can be varied due to the potential differences in the type and size of the DE particles and cellulose fibers used between these two filters which were neither discussed by literature [21] nor provided by the manufacturer. The naturally derived DE component contains porous particles that are mainly composed of silicon (Si) and can differ in shape, size, morphology, and porosity. Silica is negatively charged within a wide pH range (pH > 2) due to the presence of deprotonated silanol group (SiO^-) in its structure [10] which leads to retention of positively charged species through electrostatic interactions. Cellulosic fibers also slightly contribute to adsorbing positive species possibly through negative charges of carboxyl and hydroxyl groups in their structure [10]. These properties can explain the increased retention of the positively charged BsAb1 product on the X0HC filter at lower feed salt concentration (see Fig. 5). On the other hand, polymeric binders are positively charged which can act as an anionic exchange component through electrostatic interactions. Therefore, structural properties of different filter elements along with their composition and distribution within the filter media collectively determine the electrostatic adsorptive characteristics of the depth filters. For example, it was shown [10] that positively charged polymeric binders present in 3 M 90ZB depth filter media covers majority of the DE components leading to relatively more significant adsorption of acidic species on the filter, despite the negative charge of DE. Nevertheless,

some level of retention of basic species was also observed and attributed to their electrostatic interactions with the cellulosic fibers and DE components that remained exposed and accessible for binding. Differently, it was demonstrated [11] that basic proteins are more retained on a dual-layer PDH4 depth filter capsule than the acidic ones, perhaps due to a large surface area of DE element uncovered by the polymeric binders. Although, electrostatic adsorption on the X0HC filter seems to be minimal for the BsAb1 species in the harvest conditions, the difference in charge characteristics of the product and its variants can potentially be utilized in lower salt conditions, e.g., post-viral inactivation (VI) depth filtration, to improve the purification of target product using the X0HC filter.

The role of non-electrostatic interactions (i.e., hydrophobic and hydrogen bond) in the adsorptive properties of different depth filters has been reported in other studies [10, 11, 16]. For example, a 19% improvement in the recovery of a α-chymotrypsin model protein from the dual-layer PDH4 depth filter capsule was achieved by adding 5% ACN into flush buffer [11], which was attributed to the effect of ACN on reducing solvent polarity and increasing protein solvation. However, negligible BsAb product recovery was observed in our study using different organic solvents. This was likely due to the multimodal interactions involved between the BsAb1 molecule and the X0HC filter, where the effect of hydrophobic interactions was not the only dominant driving force for adsorption.

In a study on the adsorption of a series of peptides with varied physiochemical properties on silica nanoparticles [22], the individual contribution of electrostatic, hydrophobic, and hydrogen binding interactions was found to depend on peptide sequence and properties, surface functionality of silica particles (hydrophilicity vs. hydrophobicity), peptide concentration, and environment pH. The hydrophobic interactions with silica particles were attributed to the presence of siloxane bridge on the silica particle surface structure. In addition to the silica present in filter aids, the polymeric binder may also contribute significantly to non-electrostatic interactions, depending on its chemistry, composition, and distribution within the filter media. The binders are generally known to be hydrophobic and positively charged [15, 16]. Nevertheless, the specific impact of the polymeric binders on the non-electrostatic adsorptive properties of the X0HC filter is unclear as detailed information of the binders used is proprietary and unavailable.

The improved recovery of the BsAb1 product from the X0HC filter using arginine and urea compared with NaCl and organic solvents, when applied individually, also suggests that this BsAb1 molecule was likely retained more through the combination of mixed types of interactions rather than a single mode of dominating interactions alone. A study on the effect of urea and arginine in multimodal anion exchange chromatography found that the adsorption of proteins with a wide range of physiochemical properties was stronger than that on a strong anion exchange resin under relevant conditions due to the presence of multimodal interactions [20]. Elution modifiers, urea (2 M) or arginine (0.1 M), reduced the salt concentrations required for protein elution from multimodal anion exchange resin,

with similar effect also seen on other multimodal chromatography systems [23]. These findings are aligned with the observations in our study where arginine (1 M) resulted in higher product recovery from the X0HC filter than urea (2 M, with and without 1 M NaCl) in the post-use flush buffer because urea affects protein binding through hydrophobic and hydrogen binding interactions, whereas arginine does so via electrostatic, hydrophobic, and hydrogen binding interactions. This indicates the complex nature of the arginine-mediated interactions with the binding sites on the X0HC filter components and/or the proteins including the BsAb1 and its variants.

Furthermore, it has been reported that antibodies can go through conformational changes upon their adsorption on colloidal particles or hydrophobic surfaces, depending on protein structure and surface characteristics [24, 25]. In particular, antibodies can experience reversible conformational changes upon adsorption on HIC resins with likely more significant changes for less stable domains (e.g., Fab and CH2) [24]. Thus, upon adsorption on the X0HC filter, the BsAb1 product and its LMW variants may undergo conformational changes that likely promote stronger or even different types of interactions by exposing additional regions within the molecular structures to the filter media surface. The entropic gains achieved by these conformational changes may also play a role in making the desorption of the BsAb1 molecules less favorable [25]. The higher surface hydrophobicity and less stable structure of the LMW variants than those of the BsAb1 product likely led to more pronounced conformational alteration for the bound a-LC and a-LC dimer, resulting in their stronger adsorption on the X0HC filter than the BsAb1 product.

CONCLUSION

This work presented a case study where LMW variants of a BsAb molecule (BsAb1) were effectively reduced from the CCF material during harvest operation using a Millistak+® D0HC and X0HC depth filter train. The product-related impurities were mainly reduced by the X0HC filter with minimal retention on the D0HC filter observed. The distinct adsorptive properties of the filters were likely due to their varied binding surface area and binding sites proximity, caused by different composition or potentially different type and size of their structural elements (i.e., silica of DE filter aids as the dominant element in the X0HC filter compared with cellulosic fibers as the major component in the D0HC filter [21]). The LMW variants preferentially retained on the X0HC filter were identified to include one of the light chains present in the structure of the BsAb1 molecule (a-LC), its dimer (a-LC dimer), and a homodimer. The retention mechanism on the X0HC filter was investigated using purified BsAb1 molecule. The contribution of electrostatic interactions was minimal for the CCF material due to relatively high salt concentration, and its contribution can increase with decreasing salt concentration of the feed. It should be noted that the monomeric product had a high positive charge (+11.4) compared with the negligible positive charge of the a-LC, which can potentially be leveraged for improved

separation of these variants in conditions requiring low salt concentrations.

On the other hand, urea and arginine facilitated the product recovery from the X0HC filter (with arginine being slightly more effective), whereas different organic solvents were unable to recover any retained BsAb1 molecules. The results suggest that the BsAb1 product and its variants were retained on the X0HC filter through a complex mechanism involving a combination of different types of interactions rather than by each of these driving forces independently. Analyses of the relative surface hydrophobicity and net effective charge of the BsAb1 product and its LMW variants confirmed that the a-LC dimer and a-LC were the most hydrophobic ones, followed by the homodimer and the monomeric product (the least hydrophobic). This pattern in relative surface hydrophobicity may explain the higher tendency of the a-LC and the a-LC dimer to be retained on the X0HC filter than the BsAb1 product. Upon their adsorption on the filter media, the a-LC and a-LC dimer variants could potentially be subjected to more pronounced conformational changes than the BsAb1 product, leading to even more different adsorption favorability among these species.

In summary, this study showed that depth filtration can facilitate the removal of product-related impurities of bispecific antibody molecules with an in-depth understanding of the molecular properties of these impurities and the characteristics of the depth filters used. Although this study was focused on utilizing depth filters in CCF harvest operation, applications of these depth filters in other downstream steps (e.g., post-VI depth filtration) can also benefit from this work in assisting filter selection and process optimization to effectively reduce product-related impurities along with the other impurities. It is worth noting, however, that the contribution of the different interactions discussed here could differ with varying process conditions compared with those used in the harvest operation.

DISCLOSURE OF POTENTIAL CONFLICTS OF INTEREST
The authors declare that there is no potential conflict of interest.

DATA AVAILABILITY

Data presented in this manuscript can be available online.

ETHICS AND CONSENT STATEMENT

Consent was not required.

ANIMAL RESEARCH STATEMENT

Not applicable.

REFERENCES

1. Ma, J, Mo, Y, Tang, M *et al.* Bispecific antibodies: from research to clinical application. *Front Immunol* 2021; **12**: 626616.
2. Chen, SW, Zhang, W. Current trends and challenges in the downstream purification of bispecific antibodies. *Antib Ther* 2021; **4**: 73–88.
3. Dimasi, N, Fleming, R, Wu, H *et al.* Molecular engineering strategies and methods for the expression and purification of IgG1-based bispecific bivalent antibodies. *Methods* 2019; **154**: 77–86.
4. Guo, G, Han, J, Wang, Y *et al.* A potential downstream platform approach for WuXiBody-based IgG-like bispecific antibodies. *Protein Expr Purif* 2020; **173**: 105647.
5. Andrade, C, Arnold, L, Motabar, D *et al.* An integrated approach to aggregate control for therapeutic bispecific antibodies using an improved three column mab platform-like purification process. *Biotechnol Prog* 2019; **35**: e2720.
6. Kimerer, LK, Pabst, TM, Hunter, AK *et al.* Chromatographic behavior of bivalent bispecific antibodies on hydrophobic interaction chromatography columns. *J Chromatogr A* 2020; **1617**: 460836.
7. Manzke, O, Tesch, H, Diehl, V *et al.* Single-step purification of bispecific monoclonal antibodies for immunotherapeutic use by hydrophobic interaction chromatography. *J Immunol Methods* 1997; **208**: 65–73.
8. Tustian, AD, Endicott, C, Adams, B *et al.* Development of purification processes for fully human bispecific antibodies based upon modification of protein A binding avidity. *MAbs* 2016; **8**: 828–38.
9. Tang, J, Zhang, X, Chen, T *et al.* Removal of half antibody, hole-hole homodimer and aggregates during bispecific antibody purification using MMC ImpRes mixed-mode chromatography. *Protein Expr Purif* 2020; **167**: 105529.
10. Khanal, O, Singh, N, Traylor, SJ *et al.* Contributions of depth filter components to protein adsorption in bioprocessing. *Biotechnol Bioeng* 2018; **115**: 1938–48.
11. Nejatishahidein, N, Borujeni, EE, Roush, DJ *et al.* Effectiveness of host cell protein removal using depth filtration with a filter containing diatomaceous earth. *Biotechnol Prog* 2020; **36**: e3028.
12. Jung, SY, Nejatishahidein, N, Kim, M *et al.* Quantitative interpretation of protein breakthrough curves in small-scale depth filter modules for bioprocessing. *J Membr Sci* 2021; **627**: 1–8. 119217.
13. Nguyen, HC, Langland, AL, Amara, JP *et al.* Improved HCP reduction using a new, all-synthetic depth filtration media within an antibody purification process. *Biotechnol J* 2019; **14**: 1–11, e170071.
14. Yigzaw, Y, Piper, R, Tran, M *et al.* Exploitation of the adsorptive properties of depth filters for host cell protein removal during monoclonal antibody purification. *Biotechnol Prog* 2006; **22**: 288–96.
15. Khanal, O, Xu, XK, Singh, N *et al.* DNA retention on depth filters. *J Membr Sci* 2019; **570-571**: 464–71.
16. Yu, DQ, Mayani, M, Song, YL *et al.* Control of antibody high and low molecular weight species by depth filtration-based cell culture harvesting. *Biotechnol Bioeng* 2019; **116**: 2610–20.
17. Arakawa, T, Ejima, D, Tsumoto, K *et al.* Suppression of protein interactions by arginine: a proposed mechanism of the arginine effects. *Biophys Chem* 2007; **127**: 1–8.
18. Arakawa, T, Tsurnoto, K, Nagase, K *et al.* The effects of arginine on protein binding and elution in hydrophobic interaction and ion-exchange chromatography. *Protein Expr Purif* 2007; **54**: 110–6.
19. Shukla, D, Trout, BL. Interaction of arginine with proteins and the mechanism by which it inhibits aggregation. *J Phys Chem B* 2010; **114**: 13426–38.
20. Hou, Y, Cramer, SM. Evaluation of selectivity in multimodal anion exchange systems: a priori prediction of protein retention and examination of mobile phase modifier effects. *J Chromatogr A* 2011; **1218**: 7813–20.
21. Parau, M, Johnson, TF, Pullen, J *et al.* Analysis of fouling and breakthrough of process related impurities during depth filtration using confocal microscopy. *Biotechnol Prog* 2022; **38**: e3233.
22. Puddu, V, Perry, CC. Peptide adsorption on silica nanoparticles: evidence of hydrophobic interactions. *ACS Nano* 2012; **6**: 6356–63.
23. Hirano, A, Arakawa, T, Kameda, T. Interaction of arginine with Capto MMC in multimodal chromatography. *J Chromatogr A* 2014; **1338**: 58–66.
24. Beyer, B, Jungbauer, A. Conformational changes of antibodies upon adsorption onto hydrophobic interaction chromatography surfaces. *J Chromatogr A* 2018; **1552**: 60–6.
25. Lundqvist, M, Sethson, I, Jonsson, BH. Protein adsorption onto silica nanoparticles: conformational changes depend on the particles' curvature and the protein stability. *Langmuir* 2004; **20**: 10639–47.